

RESEARCH ARTICLE

WILEY

Design procedure for planar slotted waveguide antenna arrays with controllable sidelobe level ratio for high power microwave applications

Hilal M. El Misilmani¹  | Mohammed Al-Husseini²  | Karim Y. Kabalan³ 

¹Electrical and Computer Engineering Department, Beirut Arab University, Debbieh, Lebanon

²Beirut Research and Innovation Center, Lebanese Center for Studies and Research, Beirut, Lebanon

³Electrical and Computer Engineering Department, American University of Beirut, Beirut, Lebanon

Correspondence

Hilal M. El Misilmani, Electrical and Computer Engineering Department, Beirut Arab University, P.O. Box 11-5020 Beirut, Riad El Solh 1107 2809, Lebanon. Email: hilal.elmisilmani@iee.org

Funding information

American University of Beirut; Beirut Arab University; Beirut Research and Innovation Center

Summary

This article presents a complete design procedure for planar slotted waveguide antennas (SWA). For a desired sidelobe level ratio (SLR), the proposed method provides a pencil shape pattern with a narrow half power beamwidth, which makes the proposed system suitable for high power microwave applications. The proposed planar SWA is composed of only two layers, and uses longitudinal coupling slots rather than the conventional inclined coupling slots. For a desired SLR, the slots excitation in the radiating and feeder SWAs are calculated based on a specified distribution. Simplified closed-form equations are then used to determine the slots nonuniform displacements, for both the radiating and feeder SWAs, without the need to use optimization algorithms. Using simplified equations, the slots lengths, widths, and their distribution along the length of the radiating and feeder SWAs can be found. The feeder dimensions and slots positions are deduced from the dimensions and total number of the radiating SWAs. An 8×8 planar SWA has been designed and tested to show the validity of the proposed method. The obtained measured and simulated results are in accordance with the design objectives.

KEYWORDS

antenna arrays, high power microwave applications, slotted waveguide antennas, sidelobe level ratio

1 | INTRODUCTION

High power microwave (HPM) technology is well known in both military and commercial applications.¹ An efficient antenna to be used as the radiating system for these applications is required to have a well directive pattern, large sidelobe level ratio (SLR), and high gain. It should also have high power handling capability required to extract the HPMs from their source. Slotted waveguide antennas (SWA)² are taking a major interest in this field, with their major ability of beam pointing and HPM handling capability.³ SWAs can be also directly connected to Reltron HPM sources, without the need for additional mode converter, which makes them suitable for HPM applications. SWAs are also used in wireless technologies, maritime, and space applications.

SWAs are made of rectangular waveguides, having slots cuts used to radiate the energy.⁴ The conventional cuts have a rectangular shape. The slots can be made either on the broadwall or the narrow wall of the waveguide, with the most

This is an open access article under the terms of the Creative Commons Attribution License, which permits use, distribution and reproduction in any medium, provided the original work is properly cited.

© 2020 The Authors. *Engineering Reports* published by John Wiley & Sons, Ltd.

widely used slots are: the longitudinal broadwall slots, inclined edge or sidewall slots, and crossslots. Two types of SWAs are found, resonant and nonresonant antennas, also known as standing wave and traveling wave antennas. The resonant SWAs are preferred to their counterparts due to the short circuit termination that increases their efficiency, with no power loss and normal main beam independent of the resonance frequency, but with a narrower frequency range.^{5,6} The traveling-wave SWAs have a larger bandwidth, but suffer from lower efficiency due to the matched load used to prevent the reflections of the waves. In addition, a phase difference is present between the radiating slots, whereas, for resonant slots their impedance or admittance are real values. In this work, resonant SWAs are designed and investigated.

The design of SWAs was first presented by Stevenson and Elliott.^{5,7,8} Two main equations, based on Stevenson equations and Babinet's principle, should be solved simultaneously to determine the different slots displacements from the waveguide centerline and the slots length. Solving these equations depends on Stegen's assumption of the universality of the resonant slot length,⁹ in addition to Tai's formula¹⁰ and Oliner's length adjustment factor.¹¹ This conventional design method is complicated, and mostly rely on numerically solving several equations to deduce both the displacement and length of each slot. The excitations of the SWA individual slots, which are translated into slots displacements, control the resulting SLR of the SWA array.⁷

Pan et al¹² have presented an SWA composed of two identical narrow-wall SWAs for HPM application. Using a tunable feeding structure, the proposed antenna can be also used for beam-steering. Pan also presented another SWA with narrow-wall complementary-split-ring slots for HPM applications.¹³ Periodic air-filled corrugations have been also proposed to be added to the SWA to improve its overall gain. Sabri et al¹⁴ have presented an SWA with dual-beam directional pattern. Longitudinal slots have been made on both broadwalls of the SWA. Pulido-Mancera et al¹⁵ have proposed a technique to enhance the directivity of SWAs using metamaterial parasitic elements with discrete dipole approximation. A dual-band SWA, operating at 28 and 38 GHz, suitable for 5G applications, has been presented by Da Costa et al.¹⁶ Filgueiras et al¹⁷ have also presented an omnidirectional SWA operating at 26.2 GHz for 5G applications. Circular waveguide was used for their SWA instead of the rectangular one. An SWA with inclined slots on the narrow-wall has been proposed for beam-scanning by Tan et al.¹⁸ Lomakin et al has presented a three-dimensional (3D) printed SWA for automotive radar applications. A differential feed structure was used to couple the power to the SWA.

A major research in the SWA design field focuses on obtaining a pencil shape directive pattern, with high gain, large SLR, and narrow half power beamwidth (HPBW). The single element SWA has a relatively high gain, but suffers from the wide HPBW in the plane perpendicular to the waveguide axis. To achieve the directive pattern features, planar SWAs can be formed by stacking a specified number of radiating SWAs, fed by an additional SWA. Inclined coupling slots^{19,20} are used in the conventional planar SWA systems to couple the power from the feeder SWA to the stacked radiating SWAs. The rotation angles of these coupling slots from the waveguide centerline are either considered to be uniform or nonuniform. To control the typical inclined coupling slots, usually complicated equations that relate the inclination angle to the excitation voltage and distribution are used, which makes designing large arrays a complicated procedure.

Wu et al²¹ have presented a planar SWA operating at 140 GHz. The feeder SWA, composed of a feeding slot, overmode cavity, and the coupling slots, was designed to provide the same-magnitude but with alternating phase excitations. This was done using an integrated power divider and phase shifter. Longitudinal slots of the same lengths and offsets were also used for coupling. Kumar et al²² have proposed a planar SWA to be used in X-band. Genetic algorithm, combined with Schelkunoff's unit circle technique, have been used to synthesize the desired current distribution. The feeder was composed of two layers, the inclined coupling slot layer, and a feed layer containing a power divider. A planar SWA designed to operate at 40 GHz has been presented by Zhang et al.²³ It consisted of five different layers, for which a four-corner-fed structure with inclined coupling slots was used to suppress the sidelobe levels. The feeder was composed of an input aperture, feeding waveguide, and the coupling slots. Inclined coupling slots have been also used by Coburn et al²⁴ with one layer of feeding but with four different feeding structures to feed four 8×8 subarrays SWAs to achieve low sidelobe levels for HPM applications. Kim et al has also presented a planar SWA for HPM applications. The planar was composed of four layers: radiating slot plate, radiating waveguide, feeding waveguide, and E-plane septum divider.²⁵ It was also divided into 8×4 subarrays, each connected to multistage divider, to control the feeding to the SWA elements. Ripoll-Solano et al²⁶ have used a two-step design process with a least-square optimization approach to improve the excitation coefficients to match the desired SLR of a planar SWA. Other feeding mechanisms used complicated structures to achieve large SLR.^{27,28} In a previous work, we have also presented a planar SWA with crossshaped radiating slots to achieve circular polarization. The feeder SWA was collected at the input terminals of the radiating SWAs.¹⁹

In this work, we present a complete and efficient design procedure for planar SWAs. The proposed method uses simplified closed-form equations to determine the slots nonuniform displacements, without the need to use optimization

algorithms.^{29,30} A major contribution lies in the use of the same proposed simplified equations to design both the radiating and feeder SWAs. Longitudinal coupling slots are proposed for the feeder SWA, displaced from the waveguide feed centerline according to the desired SLR, rather than the conventional inclined coupling slots. This can provide better values of SLR. The feeder SWA is collected at the back of the radiating SWAs. Only two layers are used in the proposed planar SWA, one for the radiating SWAs, and the second for the feeding. This resulted in a simplified design when compared with the traditional planar SWA systems.

The proposed design procedure in this work is outlined as follows. For a desired resonance frequency, the slots lengths, widths, and their distribution along the length of the radiating SWAs and feeder SWA can be found. For a desired SLR, the slots excitation of the broadwall longitudinal slots for both the radiating and the feeder SWAs, are calculated from a certain distribution. The slots excitations are then used to calculate their displacements. The feeder is then coupled to the radiating SWAs in an efficient manner to obtain the required SLR. To verify the validity of the proposed design approach, an 8×8 planar SWA is designed, simulated, and then fabricated and tested. As will be shown, the results are in accordance with the design requirements, and the measured results are in good analogy with the simulated ones.

The rest of the article is organized as follows. Section 2 presents the complete design procedure steps, for both the radiating and feeder SWAs. An investigation of the mutual coupling effects that might arise in these systems is also presented in this section. Section 3 illustrates the design of a planar 8×8 SWA example. Section 4 presents the fabrication process of the presented example, along with the simulations and measurements results.

2 | DESIGN PROCEDURE

The design procedure of the planar SWA starts by determining the desired SLR and operating frequency. With these design requirements, SWAs to be used for the radiating and feeder SWAs, can be designed. The radiating SWAs are first designed. The slots shape, positions long the axis of the waveguide, length, and width, are first determined. Then, the proposed method used to find the displacements of these slots from the axis of the waveguide for a desired SLR is outlined. The feeder SWA is then designed based on the dimensions and guide wavelength of the waveguide used in the radiating SWAs. Eventually, the radiating SWAs are stacked side by side, and the feeder is coupled to the radiating SWAs. At the end of this section, the mutual coupling effects that might be found in such systems, along with ways to suppress them, are presented.

2.1 | The design of the radiating SWAs

The design of the each radiating SWA is outlined as follows. In typical situations the desired operating frequency and SLR are known. Based on the desired frequency, the waveguide inner dimensions, that is, width and height, can be found. If the desired total number of slots on each SWA is known, then using the guide wavelength of the chosen waveguide with the total number of slots, the length of the SWA can be then found. This length is calculated taking into account the spacing between the consecutive slots, in addition to the spacing between the end terminals and the first and end slot. In different situations, a limited choice of waveguides to be used as radiating SWA is found, which sets some constraints on the operating frequency, as will be seen in the illustrating example in Section 3.

In the following, the design procedure of the radiating SWAs is outlined. The slots shape and dimensions are first presented. Their positions along the waveguide broadwall are then defined. Then, the proposed method used to find the displacements of these slots from the axis of the waveguide for a desired SLR is presented. A typical SWA is sketched in Figure 1.

2.1.1 | Slot shape and dimensions

The conventional rectangular slots used in the traditional SWA design could aggravate electrical breakdown problems when working at HPMS.³¹ This is due to the enhancement of the microwave electric field which can lead to self-induced microwave breakdown of the air in the slot.³² Avoiding sharp corners is preferred in such cases. For this, round-ended slots⁹ that offer improved high power operation and easier manufacturability than the rectangular ones³³ are used in this work.

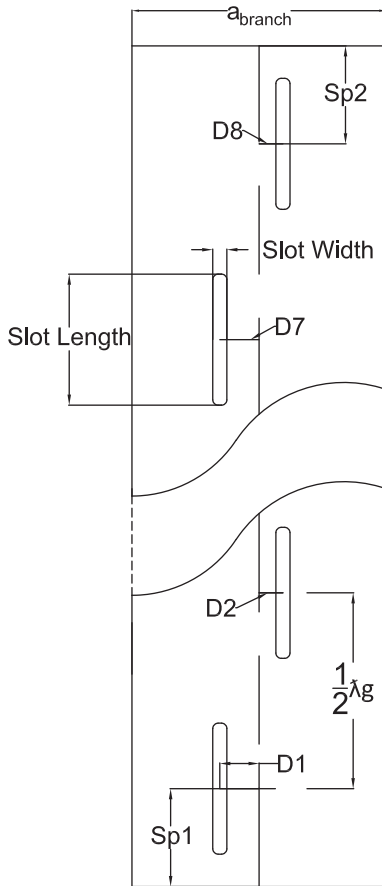


FIGURE 1 A typical SWA with eight longitudinal slots. SWA, slotted waveguide antennas

The slots length can be either nonuniform, for which the length of each slot is calculated based on optimization algorithms, or assumed to be uniform for simplicity purposes. Choosing uniform slots length can also lead to the desired results.

For optimal radiation characteristics, the length of all slots are taken to be at their resonant length. For rectangular slots,⁷ this length is typically around 0.49λ . For round-ended slots, as the one used in this work, a modification of this length is recommended. This is done as follows. The slots displacements and positions are fixed, and the length is varied starting with the typical value of 0.49λ , while checking the reflection coefficient results, till reaching an acceptable value at the desired frequency. Throughout the different designs that we have worked on using the proposed design procedure in this work, the modified round-ended slot length values differed from the typical rectangular slot lengths by 1% to 3% only.

As for the width of the slot, we have started with an initial value calculated as follows: for *X*-band SWAs, the width of a rectangular slot the mostly used in the literature is $0.0625\text{ in} = 1.5875\text{ mm}$, corresponding to $a = 0.9\text{ in} = 22.86\text{ mm}$. By proportionality,³⁰ the initial width of the slot can be computed as in (1), with a being the width of the available waveguide. Then, this width can be varied while fixing the values of the slots length and displacements, and checking the reflection coefficient results. Usually, a minor change in the width value is seen to increase the operating bandwidth.

$$\text{Slot width} = a \times \frac{0.0625\text{ in}}{0.9\text{ in}}. \quad (1)$$

2.1.2 | Slots positions

The position of the slots along the length of the SWA plays an important role in ensuring feeding the slots in phase. The phase shift between consecutive slots is determined by the electrical distance $2\pi d/\lambda_g$, with λ_g being the guide

wavelength defined as the distance traveled by the electromagnetic wave along the length of the waveguide to undergo a phase shift of 2π radians. It is calculated as in (2), with λ_0 being the free-space wavelength and c is the speed of light.

$$\lambda_g = \frac{\lambda_0}{\sqrt{1 - \left(\frac{\lambda_0}{\lambda_{\text{cutoff}}}\right)^2}} = \frac{c}{f} \times \frac{1}{\sqrt{1 - \left(\frac{c}{2af}\right)^2}}. \quad (2)$$

Using longitudinal slots, the waveguide itself acts as a transmission line. Taking a transverse electric field in each slot, the TE_{10} mode scattering is considered to be symmetrical. Using an equivalent transmission line, each slot is modeled as a shunt element. This assumption has been proved to be valid using the method of moment when the width of the slots is narrow, their offsets are not too large, and the height of the waveguide is relatively large.³⁴ Since resonant SWAs are terminated by a short circuit, open circuit impedance is found at a quarter guide wavelength down the length of the waveguide.

The slots are positioned as follows. The first and last slots are separated by a distance of $m\lambda_g/4$ from both terminals, with m being an odd number. In order to have the same input impedance viewed a $\lambda_g/4$ away, the separation between the slots is taken to be $\lambda_g/2$. In this way, all slots can be viewed as being in parallel. The shunt admittance of these terminations then vanishes at the last slot, while having the admittance of each slot to have a value of $1/N$, with N being the total number of slots. This ensures an impedance matching at the input.

2.1.3 | The slots displacements

The distance separating the waveguide broadwall centerline and the center of the slot is specified as slot displacement. Although the slots could be placed at the same distance from the centerline, it was shown in Reference 30 that such a configuration results in an SLR of around 13 dB, which is similar to the case of having equal excitations to discrete elements in an antenna array. For this, nonuniform displacements are used to design the radiating SWAs for larger SLR. Referring to Figure 1, the slots displacements are indicated by D_n , for which n is the index of each slot. To achieve higher efficiency, all slots must radiate in phase. For this, the slots are placed in an alternating order on the length of the waveguide.

Figure 2 illustrates the methodology used to calculate the slots displacements for both the radiating and the feeder SWAs. The slots displacements are calculated as follows. Starting with a desired SLR, the conductances of the slots are obtained from a certain distribution. Using the obtained slots conductances, the slots displacements can be then deduced. The slots displacements control the excitation of every slot, and hence they can be used to control the total SLR of the SWA array.

In the following, the equations of Chebyshev and Taylor distributions are given. Afterward, a gain pattern of an SWA designed using different SLR values with different distributions is given to show the validity of the proposed close-form equations.

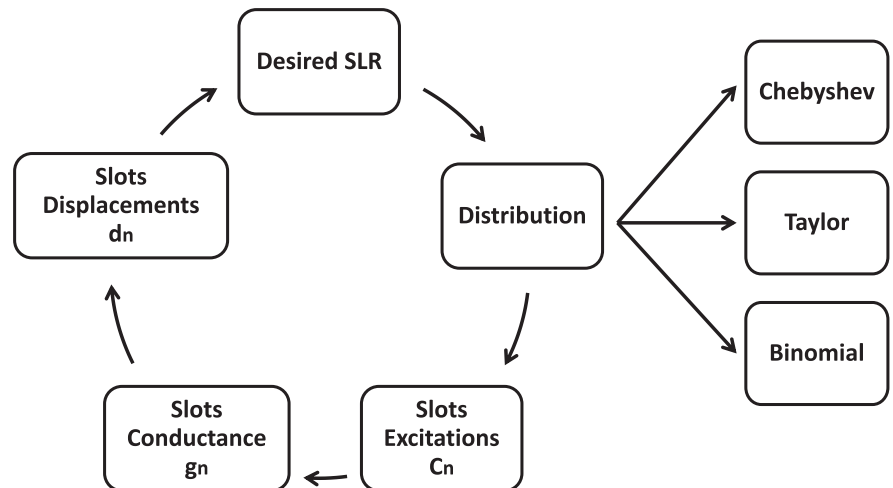


FIGURE 2 Methodology used in the calculation of the slots displacements for a desired sidelobe level ratio

Chebyshev distribution

Beginning with the equation of the array factor of a generalized Chebyshev array^{35,36} given in (3), the array factor is then calculated for a uniform spacing and an amplitude symmetrical about the center, as given in (4). The excitation coefficients can be then obtained using (5).

$$f(u) = \frac{1}{R} \prod_{n=1}^p \left(T_{N_n-1}(\gamma_n \cos \frac{u}{2}) \right), \quad (3)$$

where T_x is the Chebyshev polynomial of order x , R_n is the SLR, N_n is the number of elements, n is the index of the n th basis Chebyshev array, $\gamma_n = \cosh[\cosh^{-1}(R_n)/(N_n - 1)]$, and $u = 2\pi(d/\lambda)(\cos \theta - \cos \theta_0)$ with d being the interelement spacing and θ_0 the elevation angle of maximum radiation.

$$f(u) = \begin{cases} 2 \sum_{m=1}^{N/2} I_m \cos[(m - 1/2)u], & \text{for } N \text{ even} \\ \sum_{m=1}^{(N+1)/2} \epsilon_m I_m \cos[(m - 1)u], & \text{for } N \text{ odd} \end{cases}, \quad (4)$$

where ϵ_m equals 1 for $m = 1$ and equals 2 for $m \neq 1$.

$$I_m = \begin{cases} \frac{2}{NR} \sum_{q=1}^{N/2} f[u = p] \cos[q], & \text{for } N \text{ even} \\ \frac{1}{NR} \sum_{q=1}^{\frac{N+1}{2}} \epsilon_q f[u = v] \cos[w], & \text{for } N \text{ odd} \end{cases}, \quad (5)$$

where: $p = 2\pi/N(q - 1/2)$, $q = 2\pi/N(m - 1/2)(q - 1/2)$, $v = 2\pi/N(q - 1)$, and $w = 2\pi/N(m - 1)(q - 1)$

After calculating the slots excitations coefficients, the slots displacements can be calculated. The normalized conductance of the n th indicated by g_n can be calculated using (6) and (7),³⁰ with N being the number of slots, and c_n s are the distribution coefficients calculated using Chebyshev distribution for a desired SLR.

$$d_n = \frac{a}{\pi} \arcsin \sqrt{\frac{g_n}{2.09 \frac{\lambda_g}{\lambda_0} \frac{a}{b} \cos^2 \left(\frac{\pi \lambda_0}{2 \lambda_g} \right)}} \quad (6)$$

$$g_n = \frac{c_n}{\sum_{n=1}^N c_n}. \quad (7)$$

Taylor (one-parameter) distribution

The excitation coefficients, $I_n(z')$, for continuous line distribution of length l , are equal to:

$$I_n(z') = \begin{cases} J_0 \left[j\pi B \sqrt{1 - \left(\frac{2z'}{l} \right)^2} \right], & \text{for } -l/2 \leq z' \leq +l/2, \\ 0, & \text{elsewhere} \end{cases}. \quad (8)$$

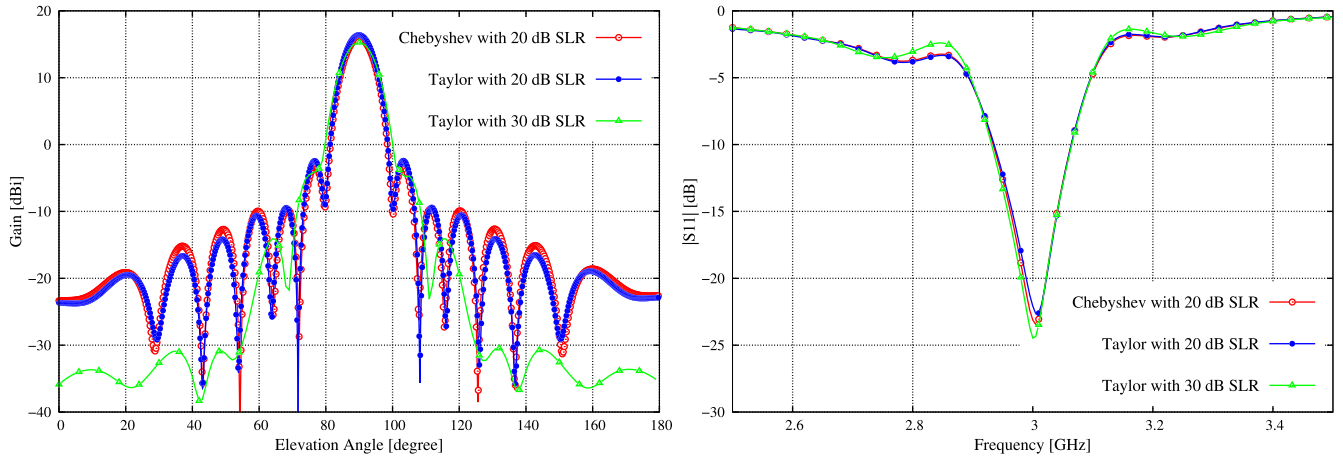


FIGURE 3 Prototype SWA: A, Gain pattern comparison, and B, $|S_{11}|$ plots, for the three different distribution cases with nonuniform displacements (using CST). SWA, slotted waveguide antennas

For the discrete case,³⁷ the current magnitudes of an N -element linear array with symmetric excitation are equal to:

$$a_m = \begin{cases} I_0 \left[\beta \sqrt{1 - \left(\frac{m-0.5}{M-0.5} \right)^2} \right], & \text{for } N = 2M \\ I_0 \left[\beta \sqrt{1 - \left(\frac{m-1}{M-1} \right)^2} \right], & \text{for } N = 2M - 1 \end{cases} \quad (9)$$

with $1 \leq m \leq M$, a_1 is the excitation of the array's center element(s), and a_M is that of the two edge elements.

Using the different distribution coefficients detailed here, we have used the close-form equation to design a prototype SWA operating at 3 GHz, using the outlined design procedure, and for the following distributions and SLR values: Chebyshev distribution with 20 dB SLR, and Taylor (One-Parameter) Distribution with 20 and 30 dB SLR. Figure 3 shows the obtained gain patterns and reflection coefficients results for the three different cases. It clearly shows that SLR design specifications in each case has been obtained, with the SWA retaining resonance at 3 GHz, despite the different slots displacements used with every distribution.

2.2 | Design of feeder SWA

2.2.1 | Feeder SWA design

The design procedure of the feeder SWA starts by obtaining its required dimensions. Referring to Figure 4, in order to place the longitudinal coupling slots of the feeder SWA centered at the centerline of every radiating SWA, the separating distance between two consecutive coupling slots must be equal to the inner width of the radiating SWA ($a_{\text{radiating}}$), in addition to twice the dimension of the wall thickness of each radiating SWA (W). Referring to the design procedure presented in Section 2.1, the distance separating two consecutive slots on the feeder must be equal to $\lambda_g/2$ for highest efficiency. As such, the guide wavelength of feeder SWA ($\lambda_{g(\text{feed})}$) should be as close as possible to twice the distance separating two consecutive coupling slots ($a_{\text{branch}} + 2 \times W$).

After obtaining the waveguide dimensions and $\lambda_{g(\text{feed})}$, the design steps follow the same design procedure of the radiating SWAs as outlined in Section 2.1. The slot length is to be calculated based on $\lambda_{g(\text{feed})}$. The first and last slot are separated from the end terminals by $m\lambda_{g(\text{feed})}/4$ with m being an odd number, and the consecutive coupling slots are separated by $\lambda_{g(\text{feed})}/2$.

Once the feeder SWA is designed, the eight radiating SWAs are stacked side by side, and the feeder SWA is collected at the bottom of the their broadwall faces. It is observed in this manner that the coupling slots are not properly placed at an equidistant from the neighboring radiating slots on each radiating SWA. This might affect the radiation pattern of

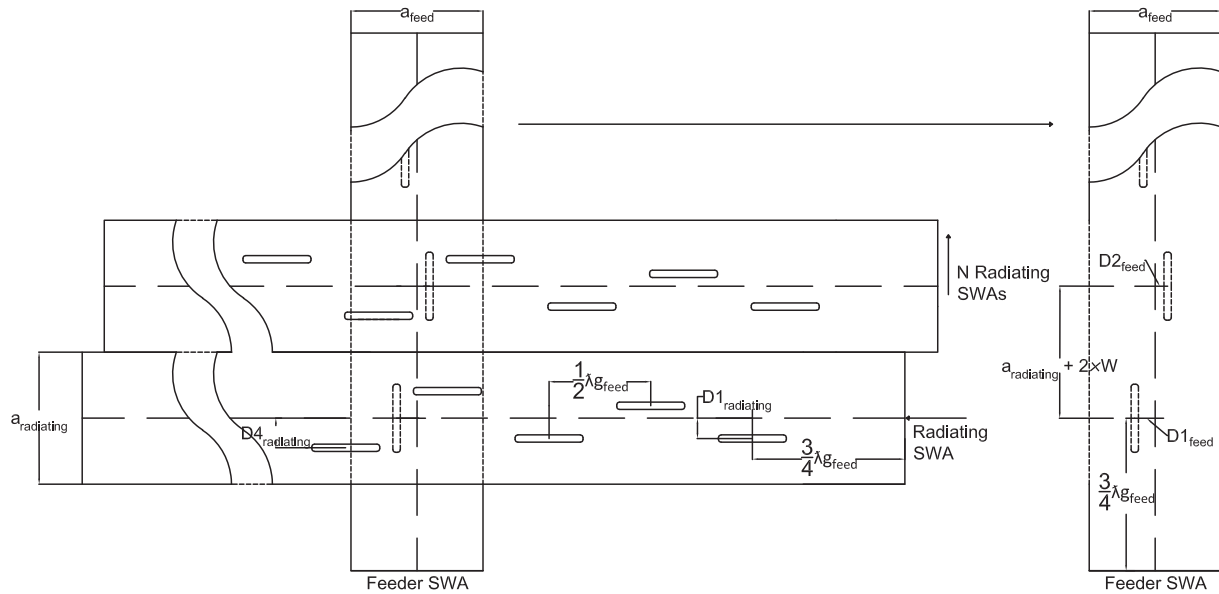


FIGURE 4 Planar SWA design showing only two radiating SWAs with the feeder SWA. $D_{\text{radiating}}$ refers to the displacement of each radiating slot from the radiating SWA centerline. D_{feed} refers to the displacement of each coupling slot from the feeder SWA centerline. W refers to the wall thickness of all SWAs. Each radiating SWA is moved by D_{feed} as per the displacement of the coupling slot feeding it. SWA, slotted waveguide antennas

the complete system, through increasing the grating lobes and hence decreasing the SLR of the system. For this, each radiating SWA is repositioned as per the displacement of its corresponding feeding slot, as shown in Figure 4.

2.3 | Mutual coupling suppression

In such systems, two different mutual coupling effects can arise. The first is due to the coupling between the radiating slots on the broadwall of the radiating SWAs (branchlines). The second is due to the coupling between the coupling slots and the radiating slots. Both of these effects have been suppressed and hence neglected in the equations as outlined in the following.

2.3.1 | Mutual coupling between the radiating slots

This type of coupling is mainly affected by the separating distance between the shunt slots, and their location on the waveguide broadwall. Their separating distance has been investigated in several articles, for which it was shown that the mutual coupling is much smaller when the slots are separated by half-waveguide length. In fact, it was concluded in Reference 38 that this type of mutual coupling can be neglected if this distance is adopted between the slots. In Reference 39, it was also shown that this type of mutual coupling can be also neglected in the design of shunt slot arrays, unless the SWA has a short length and few lots.

For SWAs, and as described in Section 2.1, the driving impedance of the radiating slots depends on their excitation, position, and displacement along the length of the waveguide, with respect to neighboring slots. For this, the procedure presented in this work mainly focuses on calculating the elements excitations for optimized radiation. These excitations, in their turn, control the displacement of each slot, and hence the coupling between the elements. The distance separating any consecutive radiating slots is chosen to have the least mutual coupling in between. The slots are also separated by half guide wavelength in each branchline SWA and feeder SWA, and placed in an alternating order for maximum efficiency and to suppress the mutual coupling between neighboring slots. Nevertheless, the mutual coupling between the neighboring slots in the same radiating SWA is not necessarily negligible in all designs, and this will be investigated in further work.

2.3.2 | Mutual coupling between the coupling and radiating slots

The coupling effect between two antennas is commonly modeled as an impedance variation. When mutual coupling is present in SWAs, it generally results in an increase of 8% in slot conductance.³⁹ The effect of mutual coupling in such designs can be simplified as follows. The resonant slot length might be affected and could result in a shift of the resonance frequency to a higher value, the impedance bandwidth (VSWR) is shifted to a higher frequency in the SWA branchlines (radiating SWAs), whereas in the feeder SWA the voltage standing wave ratio (VSWR) is shifted to a lower frequency. The combination of these effects could still lead to results as desired.

The effect of the mutual coupling on the radiation pattern and the reflection coefficient results for SWAs have been presented in several articles, for which some of them have neglected this effect,^{7,9,24,39-45} which is a valid assumption for resonant slotted arrays.⁴⁶ It was shown in Reference 44 that the effect of mutual coupling on the array performance is minimal. In Reference 34, it was concluded that the effects of higher order internal coupling modes can be ignored for full- and half-height guide. In Reference 45, it was shown that this type of coupling is only significant for small offsets or tilts.

In this work, the input to each radiating SWA, that is, each coupling slot, is located at a distance of $\lambda_g/4$ from the radiating slots to the left and to the right, as seen in Figure 4. Doing this, the impedance to the left and right of the input is transformed through quarter-wavelength sections and hence should have the same normalized values. In addition, the inner dimension, b , of the feeder, is chosen to be relatively large, and hence the internal higher order mode coupling between adjacent slots can be ignored.³⁴ For the planar SWA, the distance separating the radiating slots between the nearest SWA branchlines is larger than half wavelength, as such the mutual coupling between the slots in different SWA branchlines is negligible.²⁴

In addition, some work showed that the analytical results in the case of considering the mutual coupling in the calculations of the slots excitations are very close to those resulting from CST simulation software.^{40,47,48} Taking into account the mutual coupling effects, the radiation characteristics can be slightly enhanced in terms of the SLLs and return loss. In this work, we were able to achieve the desired SLL at the required resonance frequency, and hence any further enhancement that can result from including the mutual coupling effects in the design equations is not essential for the overall results. Nevertheless, CST simulation software is used in the simulations of this work which takes into account the effects of mutual coupling in the computational evaluation. Inspecting the results achieved in this article in later sections, even with the mutual coupling not taken into account in the calculations, the results turned out to have good analogy with the design requirements and specifications.

3 | ILLUSTRATING EXAMPLE

Due to some constraints, a we had some limitations related to the design of the radiating SWAs to be used for fabrication. Several nonstandard waveguides to be used as radiating SWAs were only found with following dimensions: $a = 5.6 \text{ cm} = 2.204 \text{ in}$, $b = 1.6 \text{ cm} = 0.63 \text{ in}$, with a wall thickness of 2 mm. These dimensions put some limits on the choice of the operating frequency that can be used for the planar SWA. For this, a frequency of 3.952 GHz is chosen, which is known in the maritime applications, one of the applications of SWAs. The rest of the design requirements are as follows: a desired SLR of not less than 20 dB is required, with eight slots on each SWA, and eight radiating SWAs, hence resulting in an 8×8 planar SWA.

Starting with the design procedure, knowing the waveguide dimensions to be used for the radiating SWAs, in addition to the desired operating frequency, λ_g is calculated to be 103.36 mm. With this value of λ_g , each radiating SWA is designed to have a total length of $5\lambda_g$. Using the design procedure presented in Section 2.1, the optimized slots length and width are found to be 37.1 mm ($\approx 0.477\lambda$) and 5 mm ($\approx 0.066\lambda$), respectively. The slots are distributed along the waveguide as discussed in Section 2.1.2. The first and last slot are chosen to be separated by $3\lambda_g/4$ from the end terminals, with the succeeding slots separated by $\lambda_g/2$. Using Chebyshev distribution, with a desired SLR of 20 dB, the slots displacements are calculated using the equations provided in Section 2.1.3, and they are listed in Table 1, second column.

As for the feeder SWA, for the illustrating example, the distance separating two consecutive coupling slots is 60 mm ($\approx 0.79\lambda$). Hence, the closest waveguide having a guide wavelength as close as possible to 120 mm ($\approx 1.58\lambda$) at 3.952 GHz is the WR-187 waveguide, having a guide wavelength $\lambda_{g(\text{feed})}$ of 125.78 mm ($\approx 1.66\lambda$), with inner dimensions of: $a = 4.75 \text{ cm} = 1.872 \text{ in}$, $b = 2.214 \text{ cm} = 0.872 \text{ in}$. It is worth mentioning here that a nonstandard waveguide could be also fabricated

with the needed guide wavelength, but the WR-187, which has close specifications to the required ones, has been chosen for fabrication due to its availability.

The feeder SWA is designed in the same procedure illustrated in Section 2.1, with eight slots made on its broadwall. The slot length of the feeder has been also optimized and found to be equal to 38 mm ($\approx 0.5\lambda$). The width of the slot is taken also to be 5 mm ($\approx 0.066\lambda$). The first and last slot are separated from the end terminals by $3\lambda_{g(\text{feeder})}/4$, and the consecutive coupling slots are separate by $\lambda_{g(\text{feeder})}/2$. Using Chebyshev distribution, with a desired SLR of 20 dB, the slots displacements on the feeder SWA, indicated by D_{feed} in Figure 4, are calculated using the equations provided in Section 2.1.3, and they are listed in Table 1, third column.

4 | SIMULATIONS AND MEASUREMENTS RESULTS

The designed planar SWA has been simulated using CST. The computed SLR, HPBW, and the gain in E- and H-planes are listed in Table 2, with the 3D gain pattern plot shown in Figure 5. As can be inspected, a pencil shape pattern has been attained, with an SLR in both planes of not less than 20 dB, with narrow HPBW, suitable for HPM applications. Lower sidelobe levels can be easily obtained if the desired SLR used to find the slots displacements is made larger than 20 dB.

The illustrating example has been also fabricated as follows. The Feeder SWA and the eight radiating SWAs are first fabricated. CNC HAAS VF-6 three axis milling machine with a precision of 0.001 mm has been used to drill the slots using a 3 mm type carbide. The eight radiating SWAs are then stacked side by side, before moving each one, upward or downward, according the displacement of the coupling slot. The eight moved radiating SWAs are then collected using a

Slot number	Displacement (mm)	
	SWA branchlines (WR-229)	SWA feeder (WR-187)
1 & 8	2.78	1.88
2 & 7	4.36	2.94
3 & 6	5.71	3.85
4 & 5	6.48	4.36

TABLE 1 Slot displacements in radiating and feeder SWAs for the 8×8 planar SWA example

Abbreviation: SWA, slotted waveguide antennas.

Antenna	E-plane		H-plane		Gain (dB)
	SLR	HPBW	SLR	HPBW	
8×8 planar SWA	22.3 dB	9.6°	28.1 dB	11.4°	24.6

TABLE 2 Simulated results of the 8×8 planar SWA example

Abbreviations: HPBW, half power beamwidth; SLR, sidelobe level ratio; SWA, slotted waveguide antennas.

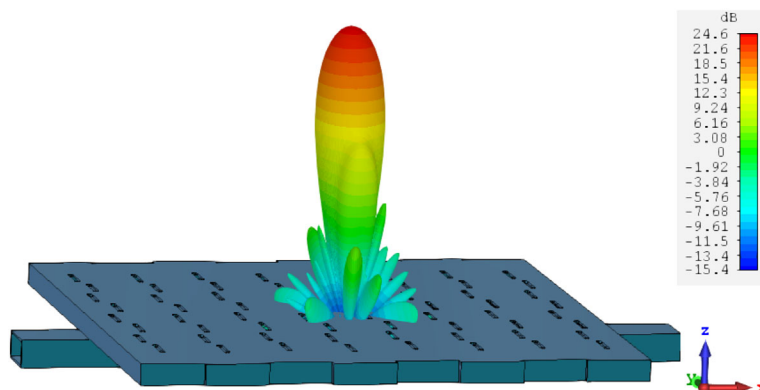


FIGURE 5 Three-dimensional simulated gain pattern plot of the 8×8 planar SWA example. SWA, slotted waveguide antennas

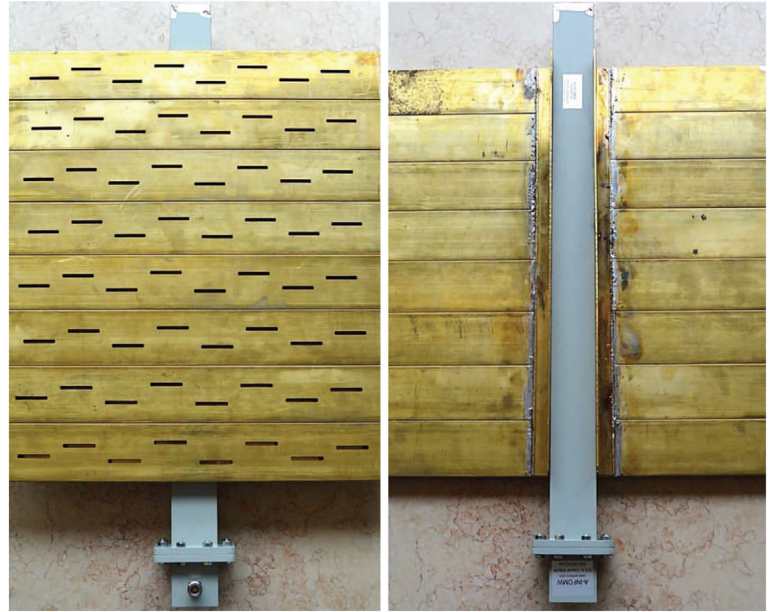


FIGURE 6 Fabricated 8×8 planar SWA, (left) front view, (right) back view. SWA, slotted waveguide antennas

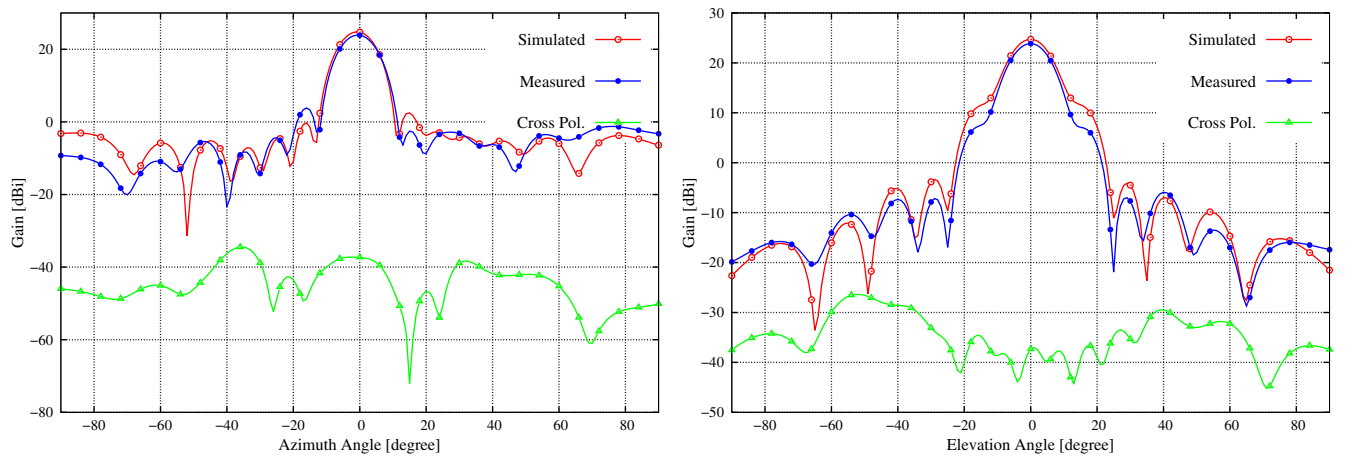


FIGURE 7 Gain pattern comparison of the simulated and fabricated 8×8 planar SWA. SWA, slotted waveguide antennas

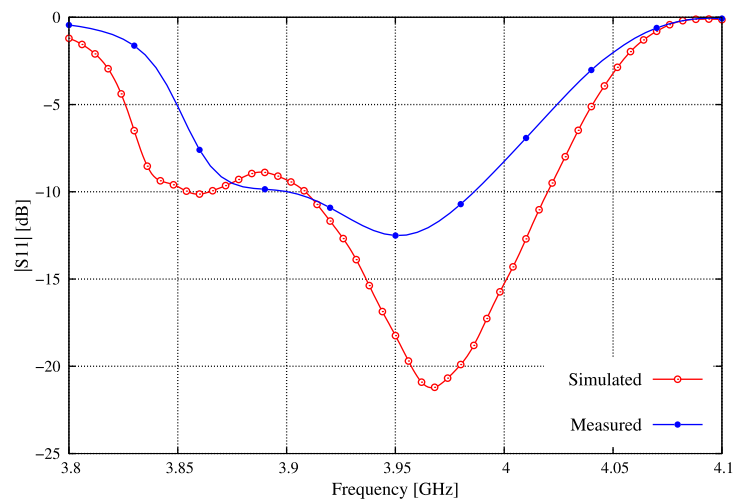


FIGURE 8 $|S_{11}|$ results comparison of the simulated and fabricated 8×8 planar SWA. SWA, slotted waveguide antennas

glue. The feeder SWA is then attached to the radiating SWAs, and welded using L-shaped copper corners on the back of the radiating SWAs. The fabricated planar SWA is shown in Figure 6.

The simulated gain pattern results are compared with the measured ones in Figure 7. The measured reflection coefficient results are also compared with those simulated using CST in Figure 8. As can be seen, the obtained measured results are very close to the simulated ones, and they are also in accordance with the design objectives.

The breakdown capability of this antenna array has been also studied. The maximum value of the voltage has been calculated on the slot responsible for the maximum radiation. The slots that give the maximum radiation are the slots found in the middle of the array system: having the maximum fed power input from the SWA feeder, and the maximum displacements from the SWA branchline centerline where the slots are located. Simulating the design taking a high input power to the feeder SWA of a 6.25 MW, the maximum voltage on these slots is found to be equal to 5.55×10^5 V/m. This maximum voltage is still lower than the onset of air breakdown 3×10^6 V/m that can cause the air to begin to break down. A lower value of this maximum voltage, and hence a higher value of power radiated, can be attained using larger slot width value, if needed.

5 | CONCLUSION

This article presented a complete design procedure of planar SWA arrays with controllable large SLR, and a pencil shape pattern, suitable for HPM applications. Longitudinal slots made on the broadwall of the waveguides are used for coupling the wave and radiating it. The procedure starts by designing the radiating SWAs taking as input the desired SLR, resonance frequency, total number of radiating SWAs, and total number of slots made on each radiating SWA. Using the dimensions of the radiating SWAs, the feeder SWA is designed to operate at the same resonance frequency, and the same value of SLR of the radiating SWAs. Using simplified closed-form, the distribution of the slots along the length of the radiating SWAs and feeder SWA are calculated based on the slots excitation from a specified distribution. An 8×8 planar SWA illustrating example has been designed and tested to show the validity of the proposed method. The obtained measured and simulated results are in accordance with the design objectives.

ACKNOWLEDGEMENTS

This work was partially supported by the American University of Beirut, Beirut Arab University, and Beirut Research and Innovation Center.

PEER REVIEW INFORMATION

Engineering Reports thanks the anonymous reviewers for their contribution to the peer review of this work.

PEER REVIEW

The peer review history for this article is available at <https://publons.com/publon/10.1002/eng2.12255>.

AUTHOR CONTRIBUTIONS

Hilal M. El Misilmani contributed to the Conceptualization-Equal, Data curation-Lead, Formal analysis-Equal, Investigation-Lead, Methodology-Lead, Project administration-Equal, Software-Lead, Supervision-Equal, Validation-Equal, Visualization-Lead, Writing-original draft-Lead, Writing-review & editing-Lead. Mohammed Al-Husseini contributed to the Conceptualization-Equal, Data curation-Supporting, Formal analysis-Equal, Investigation-Equal, Project administration-Equal, Supervision-Equal, Validation-Equal, Writing-original draft-Supporting, Writing-review & editing-Supporting. Karim Kabalan contributed to the Conceptualization-Equal, Formal analysis-Equal, Funding acquisition-Lead, Investigation-Equal, Project administration-Equal, Supervision-Equal, Validation-Equal, Writing-original draft-Supporting, Writing-review & editing-Supporting.

CONFLICT OF INTEREST

The authors declare no potential conflict of interests.

ORCID

Hilal M. El Misilmani  <https://orcid.org/0000-0003-1370-8799>

Mohammed Al-Husseini  <https://orcid.org/0000-0001-5849-0872>

Karim Y. Kabalan  <https://orcid.org/0000-0002-4494-9395>

REFERENCES

1. Rueggeberg W. A multislot waveguide antenna for high-powered microwave heating systems. *IEEE Trans Ind Appl*. 1980;6:809-813.
2. Gilbert RA, Volakis JL. Waveguide slot antenna arrays. *Antenna Eng Handbook*. 2007;9:14.
3. Mailloux RJ. *Phased Array Antenna Handbook*. Massachusetts: Artech house; 2017.
4. Lo YT, Lee SW. *Antenna Handbook: Theory, Applications, and Design*. Germany: Springer Science & Business Media; 2013.
5. Elliott R, Kurtz L. The design of small slot arrays. *IEEE Trans Antennas Propag*. 1978;26(2):214-219.
6. Elliott R. On the design of traveling-wave-fed longitudinal shunt slot arrays. *IEEE Trans Antennas Propag*. 1979;27(5):717-720.
7. Stevenson AF. Theory of slots in rectangular wave-guides. *J Appl Phys*. 1948;19(1):24-38.
8. Elliott RS. An improved design procedure for small arrays of shunt slots. *IEEE Trans Antennas Propag*. 1983;31(1):48-53.
9. Stegen RJ. Longitudinal shunt slot characteristics. *Hughes aircraft co culver city ca research and development div*. Tucson, Arizona: Hughes Aircraft Co Culver City Ca Research and Development Div; 1951.
10. Tai CT. Characteristics of linear antenna elements. *Antenna Engineering Handbook*. Pennsylvania, NY: McGraw-Hill; 1961:3-8.
11. Oliner A. The impedance properties of narrow radiating slots in the broad face of rectangular waveguide: Part I—theory. *IRE Trans Antennas Propag*. 1957;5(1):4-11.
12. Pan X, Christodoulou CG. A narrow-wall slotted waveguide antenna array for high power applications. Paper presented at: Proceedings of the 2014 IEEE Antennas and Propagation Society International Symposium (APSURSI); 2014:1493-1494; Memphis, TN: IEEE.
13. Pan Xuyuan. *A Narrow-wall Complementary-split-ring Slotted Waveguide Antenna for High-power-microwave Applications*. Mexico: Dissertation, Digital Repository, the University of New Mexico; 2018. https://digitalrepository.unm.edu/ece_etds/444.
14. Sabri MW, Murad NA, Rahim MKA. Highly directive 3D-printed dual-beam waveguide slotted antennas for millimeter-wave applications. *Microw Opt Technol Lett*. 2019;61(6):1566-1573.
15. Pulido-Mancera LM, Zvolensky T, Imani MF, Bowen PT, Valayil M, Smith DR. Discrete dipole approximation applied to highly directive slotted waveguide antennas. *IEEE Antennas Wirel Propag Lett*. 2016;15:1823-1826.
16. Costa IF, Cerqueira S Arismar, SDH. Dual-band slotted waveguide antenna array for adaptive mm-wave 5G networks. Paper presented at: Proceedings of the 2017 11th European Conference on Antennas and Propagation; 2017:1322-1325; Paris, France: IEEE.
17. Filgueiras HRD, Costa IF, Cerqueira A, Kelly JR, Xiao P. A novel approach for designing omnidirectional slotted-waveguide antenna arrays. Paper presented at: Proceedings of the 2018 International Conference on Electromagnetics in Advanced Applications (ICEAA 2018); 2018:64-67; Cartagena des Indias, Colombia: IEEE.
18. Tan L, Zhang J, Wang W, Xu J. Design of a W-band one-dimensional beam scanning slotted waveguide antenna with narrow beam and low side lobe. Paper presented at: Proceedings of the 2017 Progress in Electromagnetics Research Symposium-Spring; 2017:3625-3628; St. Petersburg, Russia: IEEE.
19. Le Sage GP. 3D printed waveguide slot array antennas. *IEEE Access*. 2016;4:1258-1265.
20. El Misilmani HM, Al-Husseini M, Kabalan KY. Simple design procedure for 2D SWAs with specified sidelobe levels and inclined coupling slots. 4th Advanced Electromagnetic Symposium (AES 2016), Spain; 2016.
21. Wu Y-W, Hao Z-C, Miao Z-W, Hong W, Hong J. A 140 GHz high efficiency slotted waveguide antenna using a low loss feeding network. *IEEE Antennas Wirel Propag Lett*. 2019;19(1): 94-98.
22. Kumar P, Kedar A, Singh AK. Design and development of low-cost low sidelobe level slotted waveguide antenna array in X-band. *IEEE Trans Antennas Propag*. 2015;63(11):4723-4731.
23. Zhang M, Hirokawa J, Ando M. A four-corner-fed double-layer waveguide slot array with low sidelobes developed for a 40 GHz-band DDD system. *IEEE Trans Antennas Propag*. 2016;64(5):2005-2010.
24. Coburn W, Litz M, Miletta J, Tesny N, Dilks L, King B. *A Slotted-Waveguide Array for High-Power Microwave Transmission*. MD: Army Research Lab Adelphi MD; 2001.
25. Kim TH, Han JH, Ryu SK. Multi-stage slotted waveguide array antenna for high power applications. Paper presented at: Proceedings of the 2019 International Vacuum Electronics Conference (IVEC), Busan, Korea (South); 2019:1-2; IEEE.
26. Ripoll-Solano L, Torres-Herrera L, Sierra-Pérez M. Design, simulation and optimization of a slotted waveguide array with central feed and low sidelobes. Paper presented at: Proceedings of the 2018 IEEE-APS Topical Conference on Antennas and Propagation in Wireless Communications (APWC 2018); 2018:886-889; Cartagena des Indias, Colombia: IEEE.
27. Qin L, Lu Y, You Q, Wang Y, Huang J, Gardner P. Millimeter-wave slotted waveguide array with unequal beamwidths and low sidelobe levels for vehicle radars and communications. *IEEE Trans Veh Technol*. 2018;67(11):10574-10582.
28. Watarai Y, Zhang M, Hirokawa J, Ando M. Sidelobe suppression in a corporate-feed double-layer waveguide slot array antenna. Paper presented at: Proceedings of the International Symposium on Antennas and Propagation (ISAP 2011); October 26, 2011; Korea.
29. El Misilmani HM, Kabalan KY, El-Hajj A, Al-Husseini M. Design procedure for 2D slotted waveguide antenna with controllable sidelobe level. 2015 IEEE International Symposium on Antennas and Propagation & USNC/URSI National Radio Science Meeting, Vancouver, BC; 2015:216-217. <https://doi.org/10.1109/APS.2015.7304494>.
30. El Misilmani HM, Al-Husseini M, Mervat MY. Design of slotted waveguide antennas with low sidelobes for high power microwave applications Progress. *Electromag Res*. 2015;56:15-28.
31. Jordan U, Anderson D, Backstrom M, Kim AV, Lisak M, Lundén O. Microwave breakdown in slots. *IEEE Trans Plasma Sci*. 2004;32(6):2250-2262.

32. Baum CE. Sidewall waveguide slot antenna for high power. *Sens Simulat Notes Note*. 2005;503. Available at: <http://ece-research.unm.edu/summa/notes/SSN/Note503.pdf>.
33. Stančulović S. *Theoretical Synthesis and Experimental Measurements of Slotted Waveguide Feeding Systems for 2.45 Ghz Industrial Microwave Heating Installations*. Karlsruhe: Forschungszentrum Karlsruhe; 2006.
34. Elliott RS, O'loughlin WR. The design of slot arrays including internal mutual coupling. *IEEE Trans Antennas Propag*. 1986;34(9):1149-1154.
35. Safaai-Jazi A. A new formulation for the design of Chebyshev arrays. *IEEE Trans Antennas Propag*. 1994;42(3):439-443.
36. El-Hajj A, Kabalan KY, Al-Husseini M. Generalized chebyshev arrays. *Radio Sci*. 2005;40(3):1-8.
37. Kabalan KY, El-Hajj A, Al-Husseini M. Bessel planar arrays. *Radio Sci*. 2004;39(1):1-9.
38. Kay A, Simmons A. Mutual coupling of shunt slots. *IRE Trans Antennas Propag*. 1960;8(4):389-400.
39. Ehrlich MJ, Short J. Mutual coupling considerations in linear-slot array design. *Proc IRE*. 1954;42(6):956-961.
40. Sekretarov S, Vavriv DM. A wideband slotted waveguide antenna array for SAR systems. *Prog Electromagn Res*. 2010;11:165-176.
41. Gruenberg H. Theory of wave-guide-fed slots radiating into parallel-plate regions. *J Appl Phys*. 1952;23(7):733-737.
42. Cullen AL. Laterally displaced slot in rectangular waveguide. *Wireless Eng*. 1949;3-10.
43. Kaminow IP, Stegen W, Robert J. *Waveguide Slot Array Design*. Culver, El Segundo and Westchester: Hughes Aircraft Company, Microwave Laboratory, Research and Development; 1954.
44. Coetzee JC, Joubert J. The effect of the inclusion of higher order internal coupling on waveguide slot array performance. *Microw Opt Technol Lett*. 1998;17(2):76-81.
45. Rengarajan SR. Higher order mode coupling effects in the feeding waveguide of a planar slot array. *IEEE Trans Microwav Theory Techniq*. 1991;39(7):1219-1223.
46. Voskresenskiy DI. Radio and Sviaz. *Antennas and Microwave Devices (Design of the Phase Antenna Arrays)*. Moscow : Radio and communication; 1981.432
47. Montesinos-Ortego I, Sierra-Pérez M, Zhang M, Hirokawa J, Ando M. Mutual coupling in longitudinal arrays of compound slots. *Prog Electromagn Res*. 2013;46:59-78.
48. Grabowski M. Non-resonant slotted waveguide antenna design method. *High Frequ Electron*. 2012;11:32-46.

AUTHOR BIOGRAPHIES



Hilal M. El Misilmani was born in Beirut, Lebanon in 1987. He received the B.E degree in communications and electronics engineering from Beirut Arab University, Debbieh, Lebanon, in 2010 and the M.E and Ph.D. degrees in Electrical and Computer Engineering from the American University of Beirut, Beirut, Lebanon, in 2012 and 2015, respectively. From August 2011 to September 2012, he was a Telecommunications Engineer with Dar Al-Handasah Consultants (Shair and Partners). From September 2012 to August 2014, he was a Researcher with Beirut Research and Innovation Center. From September 2014 to May 2015 he was a Lecturer with the American University of Beirut. From June 2015 to September 2016, he was a Research Associate

with the American University of Beirut. Since September 2015, he has been an Assistant Professor with the Electrical and Computer Engineering Department, Beirut Arab University, Debbieh, Lebanon. He is the author of more than 20 articles. His research interests include the design of high power microwave antennas, slotted waveguide antennas and vlasov antennas, antenna arrays, reconfigurable antennas, circularly polarized antennas, antennas for biomedical applications, and machine learning in antenna design. Dr. El Misilmani was a recipient of Rafic Hariri Foundation Scholarship from September 2005 to June 2010, the Association of Specialization and Scientific Guidance (SSG) Scholarship from February 2006 to June 2010, the Lebanese Association for Scientific Research (LASer) scholarship from September 2013 to May 2015, and the National Council for Scientific Research (CNRS) doctoral scholarship award from 2013 to May 2015.



Mohammed Al-Husseini received his Ph.D. in Electrical and Computer Engineering in 2012 from the American University of Beirut (AUB), Beirut, Lebanon. During his Ph.D. studies, he was recipient of the Kamal Shair Ph.D. Fellowship. He is currently a lecturer at AUB and a senior researcher at Beirut Research and Innovation Center (BRIC), Beirut, Lebanon. From 2009 to 2011, he was an exchange research scholar at the University of New Mexico (UNM), Albuquerque, NM, USA. In 2013, he was also a visiting researcher at UNM. His research interests include cognitive radio, antennas and sources for high power electromagnetics, and the design and applications of antenna arrays, reconfigurable antennas, wearable antennas, metamaterials,

RF energy harvesting, and RF circuits. He is currently working on material characterization and on the use of machine

learning for the detection of underground targets. He has over 100 publications in international refereed journals and conference proceedings.



Karim Y. Kabalan was born in Jbeil, Lebanon. He received the B.S. degree in Physics from the Lebanese University in 1979, and the M.S. and Ph.D. degrees in Electrical and Computer Engineering from Syracuse University, in 1983 and 1985, respectively. During the 1986 fall semester, he was a visiting assistant professor of Electrical and Computer Engineering at Syracuse University. Currently, he is a Professor of Electrical and Computer Engineering with the Electrical and Computer Engineering Department, Faculty of Engineering and Architecture, American University of Beirut. He is the author of two copyrighted software, six book chapters, more than 100 journal articles, and more than 124 conference articles. His research interest includes Electro-

magnetic and Radio Frequency, microstrip antenna design by using sophisticated patch element and array theoretical modeling techniques, cognitive radio antenna, and MIMO antenna systems.

How to cite this article: El Misilmani HM, Al-Husseini M, Kabalan KY. Design procedure for planar slotted waveguide antenna arrays with controllable sidelobe level ratio for high power microwave applications. *Engineering Reports*. 2020;e12255. <https://doi.org/10.1002/eng2.12255>